Self-Assembled Nanoparticle-Nanotube Structures (nanoPaNTs) Based on Antenna Chemistry of Single-Walled Carbon Nanotubes

Juan G. Duque,[†,§] J. Alexander Eukel,[†] Matteo Pasquali,*[,†,‡] and Howard K. Schmidt*[,†]

Department of Chemical and Biomolecular Engineering, and Department of Chemistry, The Smalley Institute for Nanoscale Science and Technology, Rice University, 6100 South Main, MS-362, Houston, Texas 77005

Received: June 28, 2009; Revised Manuscript Received: September 1, 2009

Single-walled carbon nanotubes (SWNT) polarize readily in the presence of electromagnetic (EM) fields, enabling a variety of electrochemical reactions. Here, we study the reaction of transition metal ion salts in the presence of surfactant-stabilized SWNT individually suspended in water when activated by alternating EM fields in the radio frequency (RF), microwave (MW), and optical regimes. Atomic force microscopy (AFM) images show formation of novel SWNT nanoparticle−nanotube structures (nanoPaNTs). The resulting nanoPaNTs include SWNT with metallic nanoparticles at one or both tips ("dumbbells"), SWNT toroids, and straight SWNT "threaded" through multiple SWNT rings to form shish-kebab structures. Mixtures of surfactants and polymer apparently modify the local environment of polarized SWNT in a manner that reduces the energy needed for ring formation. We also infer that electrodeposition reactions proceed on a significantly faster time scale than ring formation. These processes can potentially be used for self-assembly of complex 3-D structures.

Introduction

Single-walled carbon nanotubes (SWNTs) are cylindrical all-carbon molecules with remarkable mechanical and electrical properties.[1−6] The high-pressure carbon monoxide (HiPco) process generates about 50 different specific SWNT (*n*,*m*) species, averaging 0.9 nm in diameter and 300−1000 nm in length.[7,8] Roughly two-thirds are semiconductors that fluoresce in the near-infrared;[4] the rest are metallic or small bandgap (∼few meV) semiconductors. Metallic SWNT (m-SWNT) are 1-D ballistic conductors and among the best electrical conductors known,[2] supporting current densities of $\sim 10^9$ A/cm^2.[3,9] Because of their high aspect ratio and conductivity, individually suspended SWNT in aqueous surfactant suspensions polarize strongly in response to external electric fields. This property enables dielectrophoresis[10−12] and antenna chemistry[13] in alternating (AC) fields. At high field strength, isolated SWNT generate steep electric field gradients around their tips[14] enabling field emission in vacuuo;[15,16] field emission has also been observed in solution, both directly by electrochemical methods[10,17] and indirectly by antenna chemistry.[13] Recent efforts have shown that individualized SWNT are promising platforms in nanomedicine for transfection,[18] magnetic resonance imaging (MRI) contrasts,[19,20] fluorescent tracking,[21] photothermal ablation,[22] and radio frequency (RF) thermoablation.[23]

Bulk SWNT absorb efficiently and convert electromagnetic (EM) radiation across a broad frequency range spanning RF,[23] microwave (MW),[24] and visible radiation[25] into heat. SWNT polarize in MW fields, acting as nanoscale antennae;[13] ionic conduction from stabilizing surfactants can also contribute to the polarization in the low frequency RF regime.[26] SWNT display optical absorptions due to resonant band-to-band transitions[4,27] and π-plasmon excitation;[28−30] however, it is not clear whether they can support antenna-like collective resonances in the optical regime. Optically driven collective resonances (surface plasmon polaritons) are well-known for certain metallic nanoparticles,[31−33] where they generate strong electric field gradients at asperities and junctions.[34,35] These effects underlie surface enhanced Raman scattering,[36] as well as shape-selective photochemistry.[34,37] Similar effects have not been reported for SWNT, even though they are excellent conductors with high extinction coefficients. Theoretical studies by Burke[38] indicate that SWNT have exceptionally high kinetic inductance, which decreases their group velocity (and thus their response frequency) to $\sim 10^6$ m/s (300 times slower than the speed of light $c = 3 \times 10^8$ m/s). Studies by Hao[39] show that SWNT with lengths in the micrometer range should polarize and display relatively sharp current resonance at low THz frequencies. This model is supported experimentally by a recent observation of ballistic electron resonance of SWNT in the THz regime.[40] Kinetic inductance depends on diameter and carrier density; Salahuddin et al. have shown that metallic structures over about 10 nm in diameter should have group velocities close to the speed of light;[41] this is supported by Ren's experimental observation of resonant scattering by multi-walled carbon nanotubes (MWNT) in the visible regime.[42]

Individually dispersed SWNT display rich electrochemistry, as evidenced by selective electron transfer reactions[43−47] and photochemical processes.[48,49] We recently showed that HiPco SWNT individually suspended in anionic surfactants (dodecylbenzenesulfonic acid, sodium salt; SDBS) display preferential activation of m-SWNT by MW fields and develop substantial electrochemical current densities at their tips—antenna-like behavior[13]—and drive electrodeposition reactions with transition metal salts at near diffusion-limited rates forming novel nanostructures. Similarly, Warakulwit et al. have demonstrated deposition of palladium at the tips of bundles of supported MWNT using a pulsed bipolar electrochemical method.[50] Carbon nanotube (CNT) nanostructures—such as metallic nanoparticle decoration[13,50−52] and rings[53−58]—have been obtained and

* To whom correspondence should be addressed. E-mail: hks@rice.edu (H.K.S.); mp@rice.edu (M.P.).
† Department of Chemical and Biomolecular Engineering.
‡ Department of Chemistry.
§ Currently at Los Alamos National Laboratory, Los Alamos, NM 87545.

10.1021/jp906038k CCC: $40.75
Published on Web 10/07/2009

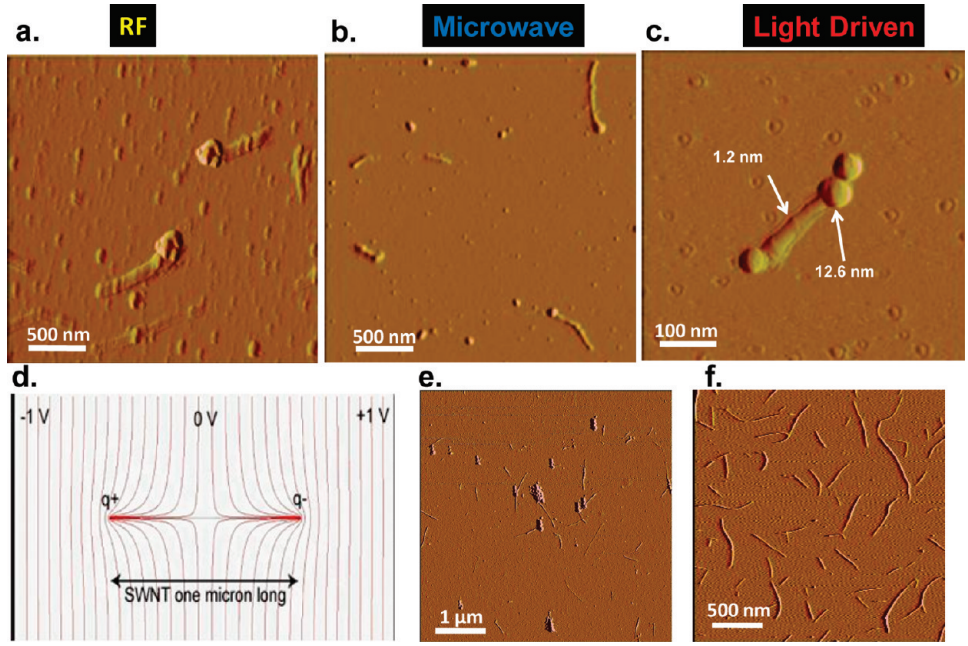

Figure 1. (a−c) Representative AFM images of selective tip deposition of metallic nanoparticles at the end of a SWNT using RF (a), MW (b), and broadband optical radiation (c). (d) Illustration of a 1 μm metallic SWNT under applied EM. (e) Extended broadband optical radiation (2 h). (f) As-prepared SWNT suspension (after sonication); rings and rackets are absent from these samples.

studied for several years. Nanotube/nanoparticle hybrids of indiscriminate[51,52] or end-selective nanoparticle deposition[13,50] have been reported. CNT rings were obtained as a direct result of growth conditions,[54] organic reactions,[57] molecular templates,[59] and ultrasonication procedures.[55,56]

In this work, we report physical-chemical response of surfactant-stabilized, individually suspended SWNT in water to EM fields in the RF, MW, and optical regimes. We show that SWNTs in SDBS (SDBS-SWNT) polarize under RF excitation at 2 MHz and induce the deposition of metal particles at their tips. We also find that similar deposition can be driven by broadband optical radiation (200 nm through the near IR); this suggests that, to some extent, SWNT appear to polarize axially even at optical frequencies despite their small number of available carriers (similar to results previously reported under MW fields[13]). In the presence of other species such as metal ion salts, anionic surfactants, and polymers, the polarization of SWNT in EM fields leads to the production of a variety of SWNT nanoparticle−nanotube structures (nanoPaNTs) including dumbells, toroids, and shish-kebab structures. These electric field-driven processes and their resulting nanostructures may prove to be broadly useful in electronics, photocatalysis, photovoltaics, and nanomedicine.

Results and Discussion

The interaction of SWNT with EM fields was studied on samples of raw HiPco SWNT stabilized as individuals by SDBS surfactant in water in the presence of transition metal salts (gold ($HAuCl_4$), silver ($AgNO_3$), palladium (K_2PdCl_4), platinum (H_2PtCl_6), copper ($CuCl_2$), and iron ($FeCl_3$)), and polymers (polyvinylpyrrolidone, PVP; see Experimental Section). A broad range of EM wavelengths were used, including RF (2 MHz), MW (2.54 GHz), and a broadband light (150 W high pressure mercury arc lamp, 220 nm to near IR).

We observed tip-selective deposition of gold nanoparticles from $HAuCl_4$ on SDBS-SWNT using RF excitation, similar to our previous report using MW radiation.[13] Importantly, SDBS was chosen as the surfactant because it inhibits spontaneous redox reactions between SWNT and transition metal salts.[13] Panels a and b of Figure 1 show AFM images of gold nanoparticles electrodeposited on the tips of SWNT using RF, and MW, respectively. The RF experiments were carried out on SDBS-SWNT suspensions between a pair of silicon wafer electrodes with insulating thermal oxide surfaces. The electrodes were spaced apart by 150 μm; 2 MHz RF at 150 V peak-to-peak was applied for 3 min using a Huttinger RF power supply. Similar nanoparticle electrodeposition was obtained using Pt, Pd, Fe, and Cu salts. We recently showed that HiPco SWNT individually suspended in surfactants under microwave fields at similar field strengths develop substantial electrodeposition current densities at their tips (on the order of 10^{-15} A per SWNT tip).[13] m-SWNT in electric fields maintain uniform potential along their length by rapid charge redistribution; consequently, strong electric field gradients are generated at their tips (see Figure 1d for a schematic of a 1 μm long SWNT in a 1 V/μm MW electric field). The present results indicate that electron transfer processes originally observed in the GHz regime are also operative in the low MHz regime.

Interestingly, we also found particle formation at the tips of the SWNT with Pt, Au, and Ag salts when exposed to a broadband light source (near IR to 220 nm) for 5 min. Figure 1c shows a representative AFM of the reaction products. Free-floating gold nanoparticles were generated copiously in this reaction. A few nanoparticles were found directly deposited on SWNT, and about 10% of the SWNT were so decorated. Nanoparticles found on SWNTs were concentrated at or near their tips, but this deposition was not as tip-specific as in our prior work using MW excitation.[13] Preferential nanoparticle production at the SWNT tips suggests that SWNT appears to polarize axially to some extent even at optical frequencies. Given their low carrier density and small diameter, this result is not expected based on prior theoretical reports.[39,41] Further studies are needed in order to clarify the complete mechanism of this reaction and reconcile our experimental observation with theoretical predictions. However, no particle formation was observed in suspensions of

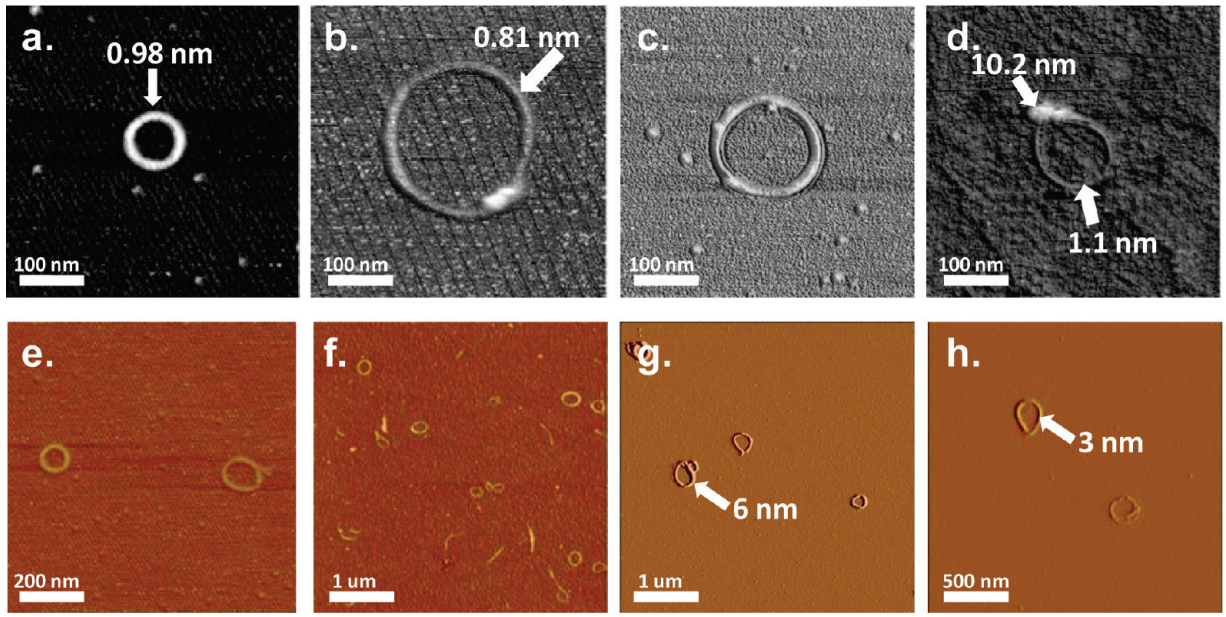

Figure 2. Representative AFM image of SWNT rings. (a−e) Individual SWNT rings. (f−h) Rings of SWNT bundles. (b−f) Rings with overlapping ends. (c−d) Rings with metallic particles on the side-walls (c) and at the ends (d). (f) Racket-like SWNT rings.

SDBS-SWNT and transition metal salts in the absence of electromagnetic radiation or as a consequence of the dispersion procedures (Figure 1f). Assembly of pre-existing nanoparticles regiospecifically with SWNT tips is indeed known, although such assembly is generally mediated by linker moieties with strong affinity to the particular nanoparticles employed.[60−64] For instance Smalley et al. induced assembly with gold nanoparticles using thiol-terminated long-chain alcohols that were in turn attached to acid-oxidized SWNT via esterification.[60] Recently, Hamilton et al. used coupling reactions to either the carboxylate or hydroxide residues of the SWNTs' open ends via piranha etching to attached FeMoc nanoparticles at the ends of SWNTs.[61] In contrast, we mixed and incubated premade gold nanoparticles and surfactant-coated SWNT without linker moieties, in the presence and absence of MW fields and looked for evidence of self-assembly with AFM, however no such assembly was found. We therefore suspect that any dangling bonds, carboxylic acids, etc. that might be present at the tips—as a result of suspension procedures—would be occluded by the surfactant, precluding nanoparticle assembly under ambient conditions (e.g., in the absence of EM fields).

In order to maintain a stable SWNT-nanoparticle suspension, PVP was added (0.25 wt %) before initial MW exposure; PVP is a well-known capping agent used to stabilize both SWNT[65] and metallic nanoparticles.[66,67] A variety of unusual nanostructures were observed after MW excitation of SWNT suspensions prepared in surfactant mixtures (SDBS+PVP). SWNT rings were formed upon MW irradiation when the surfactant composition was adjusted to 0.75 wt % SDBS and 0.25 wt % PVP. It is also important to note that the SDBS-PVP concentration and PVP molecular weight were chosen in order to maintain the optical properties and stability of the SWNT suspensions as we previously reported.[13,68] Figure 2 shows single (Figure 2a−e) and bundled (Figure 2f−h) SWNT rings with an average diameter of 125 nm. Rings were also generated in the presence of reducible transition metal salts (i.e., Au, Ag, and Cu) (Figure 2d). We found that SDS could be substituted for SDBS in the surfactant mixture without affecting the reaction. Interestingly, no rings were obtained in the absence of MW irradiation or when either surfactant was used without PVP in conjunction with MW irradiation. Experiments in the presence of metal salts sometimes led to ring-dot structures (Figure 2d) where it appears that distinct Cu particles originated at the ends of the SWNT formed first, followed by ring formation. We infer that particle formation at the SWNT tips and ring formation must occur on very different time scales. If, in fact, the ring had formed first, the tip field enhancement would have disappeared, supporting particle production or yielding nonspecific side-wall decoration of the SWNT at multiple locations. Ring formation therefore appears to be a slower and more energetic process than nanoparticle deposition, which can proceed with diffusion-limited kinetics on subsecond time scales.[13] We note that these SWNT ring-dot structures are similar to the c-shaped resonant structures discussed in the literature on negative index materials.[69] This suggests that ring-dot structures with SWNT tips separated by (insulating) metal oxide nanoparticles might have interesting EM scattering properties. Additional representative AFM images of these products at different magnifications are shown in Figure 3a−d. It can be seen that we obtained a high yield of rings with relatively small diameters. Figure 3e shows the diameter distribution of the SWNT rings (shown in Figure 3, a−d) ranging between 30 and 75 nm, with a mean diameter of 50 nm. Also shown are remarkable structures that appear to be long, unmodified SWNT "threaded" through one or more rings in shish-kebab fashion. These results may indicate type selectivity in ring formation under MW irradiation, based on our previous experimental finding of preferential activation of m-SWNT under similar operating conditions.[13] Table 1 shows a summary of the different nanostructures formed with their corresponding experimental procedures.

Although ring formation has been observed and studied in the SWNT/CNT context for several years[53−58]—as direct result of growth conditions,[54] organic reactions,[57] molecular templates,[59] and ultrasonication procedures[55,56]—this is the first reported occurrence of ring formation as a result of MW irradiation and not as a result of the suspension procedures

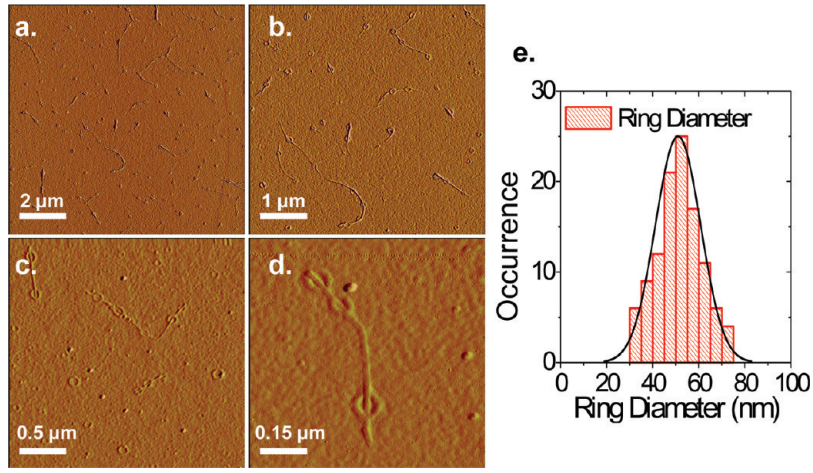

Figure 3. Representative AFM images of SWNT rings on sticks. (a−d) AFM images at 10 (a), 5 (b), 2.5 (c), and 0.75 μm (d) of SWNT rings on sticks. (e) Diameter distribution of SWNT rings for several AFM images.

TABLE 1: Summary of Nanostructures Formed and Their Corresponding Experimental Procedures

SWNT nanostructure	surfactant	electromagnetic field			notes
tip deposition	SDS SDBS	RF field (3 min)[a]	MW field (8 s)[a]	arc lamp (5 min)[b]	tip deposition was more predominant in MW reactions; arc lamp reactions resulted in free-floating particles and very small fraction of specific deposition
shish-kebab	SDBS-PVP		MW field (8 s)[c]		shish-kababs were only observed in mixtures between SDBS and PVP
ring	SDBS-PVP		MW field (8 s)[d]		rings were formed as individuals and as bundles with and without metal ions; shish-kebab rings ranged between 30 and 75 nm in diameter, isolated rings had a ring average diameter of 125 nm

[a] Metal salts used: Au, Pt, Pd, Fe, and Cu. [b] Metal salts used: Pt, Au, and Ag. [c] No metal salts were added. [d] Metal salts used: Au, Ag, Cu, and solutions without salts.

(Figure 1f). Moreover, we believe that PVP plays an important role in the ring formation in our system and the effects of concentration and molecular weight on the ring formation should be an interesting subject to explore in future work.

Ring formation is well known and understood in semiflexible filaments and molecules like DNA.[70−75] For example, it has been theoretically shown and observed experimentally that semiflexible molecules in poor solvents can undergo conformational changes to minimize solvent contact and obtain a more energetically favorable configuration, which can result in partially collapsed shapes, racket conformations, and tori.[73,75] These conformations reduce molecule−solvent contact without causing excessive bending penalties and result from the interplay between two opposite forces: the bending force related to the chain stiffness and the self-attraction. However, the metastable (unravelled) configuration is separated from the lower-energy shapes (rackets, tori) by an energy barrier. Essentially, the chain must bend into higher energy conformations before the self-attractive forces take over and drive loop closure. Normally, thermal fluctuations provide the barrier-crossing mechanism; when such thermal fluctuations are too weak compared to the bending stiffness, no conformational changes (ring formation) are observed[75] unless external forces bend the chains causing the crossing of the energy barrier. The simplest model that can effectively capture the competition of bending and self-attraction (see, e.g., Martel et al.[55] and Schnurr et al.[73,76]) is based on a semiflexible filament whose total energy U includes a bending energy U^b dependent on the bending stiffness κ, and a self-attractive energy U^a dependent on the self-attractive potential per unit length of overlapping u_0

$$U = U^b + U^a = \frac{1}{2}\kappa \int_0^L ds\left(\frac{d\theta}{ds}\right)^2 - \lambda u_0 \qquad (1)$$

where L is the length of the filament, s is arc length along the filament contour, θ is the angular position, r is the ring radius, and λ is the extent of overlap (Figure 4a). Here we have disregarded the effect of the coordination number in filaments

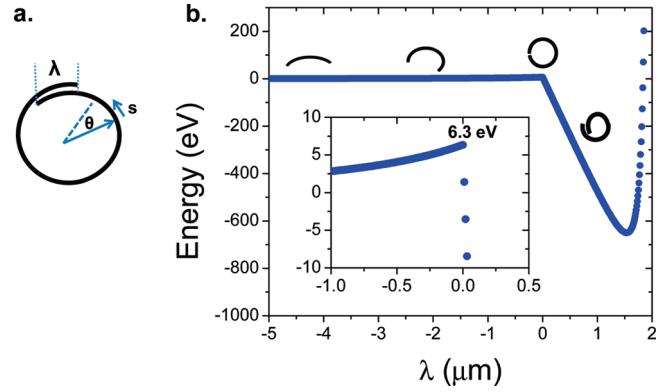

Figure 4. Self-attractive energy to induce ring formation. (a) Schematic diagram of the formation of a ring. (b) Energy barrier to induce ring formation (L_p = 25 μm, L = 2 μm, and u_o= 500 eV/ μm).

with multiple self-overlaps, which changes quantitatively (but not qualitatively) the energy of tightly wound filaments (see discussion in Schnurr et al.[76]). Assuming that the filament shape is circular (lowest curvature conformation) yields $s = \theta r$ and $\lambda = L - 2\pi r$ and the final expression of the total energy is

$$U = \frac{\kappa L}{2r^2} - (L - 2\pi r)u_0 \text{ for } 2\pi r \leq L \text{ and}$$

$$U = \frac{\kappa L}{2r^2} \text{ for } 2\pi r \geq L \quad (2)$$

Equation 2 can be used to plot an energy landscape which illustrates the energy of a chain at different stages of ring formation (Figure 4b). Clearly, the energy minimum is in the ring configuration for sufficiently strong self-attraction, as in the case of SWNTs, where the self-attractive potential per unit length of overlap is 500 eV/ μm.[77] However, in order to fold, the filament must overcome an energy barrier $U^{max} = 2\pi^2(\kappa)/(L) = 2\pi^2 k_B T(L_p)/(L)$, where k_B is Boltzmann's constant, T is temperature, and $L_p \equiv \kappa/k_B T$ is the filament persistence length. Therefore, the energy barrier can be estimated based on the SWNT persistence length. Martel et al.[55] and Yakobson and co-workers[78] computed L_p by treating SWNTs as continuum elastic cylindrical thin shells, for which $\kappa = \pi C r^3$; Martel et al. estimated $C \approx 130$ N/m on the basis of early theoretical modeling by Yakobson et al.;[78] Kudin et al.[79] later computed $C \approx 345$ N/m on the basis of ab initio calculations. Direct measurements of the persistence length of SWNT in water[80,81] show that the persistence length of typical HiPco SWNTs (diameters $\approx 0.8-1.2$ nm) range from 25 to 140 μm (i.e., $C \approx$ 680 N/m).

A relatively long, thin SWNT with $L_p = 25$ μm and $L = 2$ μm would have to overcome an energy barrier $U^{max} \approx 250 k_B T \approx 6.3$ eV before self-attraction would take over and close the ring; even using the lower theoretical estimate of persistence length of Martel yields a minimum activation energy $U^{max} \approx 50 k_B T \approx 1.3$ eV for ring formation. Clearly, the energy barrier is too high (on the scale of $k_B T$) for spontaneous activation (in fact, no rings are observed in the absence of EM fields). How the EM field is able to transmit so much energy to bend the SWNTs is not at all clear. The active ring formation mechanism must generate substantial buckling and bending forces; the attractive interactions between SDBS and PVP[68,82−86] may assist this mechanism by bridging opposite ends of a bending SWNT and therefore stabilize the intermediate configurations. We suspect that the field-induced accumulation of charge at the SWNT tips is the primary cause of the bending forces, along with corollary electrochemical and electrostatic effects and the strong interaction of the adsorbed PVP.

Although the minimum energy configuration is that of a tightly wound ring, only a small degree of overlap (tens of nm) is required to stabilize the ring conformation. Figure 2 shows rings with small overlap (e.g., 20 nm in Figure 2b) as well as racquet shapes with ~50 nm overlap (Figure 2f); these conformations are kinetically trapped states, similar to those observed in SWNT systems[55,56] and in the condensation of DNA and other semiflexible structures.

Overall, these observations suggest that the electromagnetic field induces unanticipated compressive and bending forces needed to start the process of SWNT ring formation. The PVP chains may contribute to the ensuing of such forces or lower the activation energy by bridging opposite sides of a bending SWNT. Further experimental and theoretical work is needed to explain the formation of rings driven by electromagnetic fields and assisted by the presence of PVP.

Experimental Section

Reagents. SWNT were produced via the HiPco process and used as suspensions prepared with nanopure water and surfactants including sodium dodecyl sulfate (SDS, 99%, Fisher), dodecylbenzenesulfonic acid, sodium salt (SDBS, 99%, Aldrich), and polyvinylpyrrolidone (PVP, 55 kDa, analytical grade, Aldrich). *N*-Methyl-pyrrolidone (NMP) and 2-isopropanol were obtained from Aldrich. Transition metal salts were used as received from Aldrich, including gold ($HAuCl_4$, 99.999%), silver ($AgNO_3$, 99.999%), palladium (K_2PdCl_4, 99.99%), platinum (H_2PtCl_6, 99.995%), copper ($CuCl_2$, 99.999%), and iron ($FeCl_3$, 99.99%).

SWNT Suspension Preparation. Stable suspensions of SWNT solutions were prepared by first homogenizing 250 mg of raw HiPco SWNT in 200 mL nanopure water that contained 1 wt % surfactant at 500 rpm for 2 h (Dremel Multi-Pro tool, 35 000 rpm, Racine, WI). Second, tip sonication (Cole Parmer Ultrasonic Processor, Tip- Model CV26, Vernon Hills, IL) was performed in a 20 mL water bath at 20% power for 2 min followed by bath sonication (Cole Parmer Ultrasonic Cleaner (Model 08849-00), Vernon Hills, IL) for 2 min. Third, ultracentrifugation (Sorvall Discovery 100SE (by Hitachi), Rotor - AH629, 36 mL) for 4 h at 29k RPM was followed by subsequent removal of 2/3 volume of the supernatant portion via pipet. Note that our experimental observations suggests that homogenization, low sonication time/power and temperature control of the SWNT solution are the most important steps to obtaining a suspension of SWNT suitable for EM experiments. All reactions were carried out using surfactant suspended SWNT at an initial SWNT concentration of 5 mg/L.

Images: Atomic Force Microscopy. AFM images were taken using a Nanoscope IIIa system (Digital Instruments/Veeco Metrology, Inc., Santa Barbara, CA), in tapping mode at a scan rate of 2 Hz. SWNT suspensions (20 μL) were spin coated at 3000 rpm onto a freshly cleaved mica surface (Ted Pella, Inc., Redding, CA). To remove the excess of surfactant, immediately after the SWNT solution was deposited, it was rinsed with 2 mL of 2-isopropanol, followed by 5 μL of NMP, and then again with 2 mL of 2-isopropanol after which the sample was spun for 7 min. To obtain high quality AFM images, we found that the cleaning procedure was fundamental, as well as the addition of the SWNT suspension in a continuous flow instead of dropwise. Drops cause a build-up of SWNT layers that tend to form bundle-like structures.

Formation of nanoPaNTs. nanoPaNTs were obtained using various experimental procedures and EM. Selective deposition of particles at the ends of the SWNT (dumbells) were obtained using MW, RF, and optical irradiation. The MW radiation source was a multimode microwave reactor ($MARS_X$, CEM Corporation, 2.54 GHz, Matthews, NC) programmed at 1000 W. The reactions were carried out in the center of the MW using 5 mL of SWNT suspensions and 8 s exposure time. RF low frequency radiation was provided by an AC power supply (Huttinger, 13.56 MHz, Farmington, CT). The 40 μL sample containing SWNT and Au salts was placed between two silicon oxide wafers (n-type arsenic, 3.5 μm oxide layer, Wafer World, West Palm Beach, FL) spaced 150 μm apart by a glass coverslip and exposed to 150 V for 3 min. The source of light irradiation was a mercury arc lamp (ACE glass, Near IR to 220 nm UV at 150 W, Vineland, NJ). Light-irradiated samples were exposed for 5 min. All samples were prepared from suspensions with a

SWNT concentration of 5 mg/L to which 50 μL solutions of 1 mM metal ion salts (Au, Pt, Ag, or Fe) were added. Ring structures were obtained in separate experiments that utilized a mixture of surfactants (0.75 wt % SDBS and 0.25 wt % PVP) under MW irradiation, with and without the presence of metal salts.

Conclusions

Electric fields induce solution phase electron transfer chemistry of SWNT and transition metal salts; these chemical routes, termed antenna chemistry, can lead to a variety of self-assembled nanoPaNTs: dumbells, SWNT toroids, and straight SWNT "threaded" through multiple SWNT rings (shish kebab structures). Proper surfactant selection prevents spontaneous redox reactions between SWNT and transition metal salts; the resulting nanostructures are due to electrochemical interactions between the SDBS-SWNT, transition metal salts, and the incident EM fields. SWNT rings form only under MW irradiation and when negatively charged surfactants (SDS or SDBS) are combined with PVP; they do not form as a consequence of sonication under the conditions used here to prepare the suspensions, suggesting that PVP plays a fundamental role in the ring formation. Reducible metal salts are not required for ring formation; when they are present, metal nanoparticles deposit on the SWNT before SWNT rings are formed. Although more work is needed to clarify its mechanisms, antenna chemistry is likely to provide new routes for bottom-up production of complex 3-D nanostructures. These novel nanoPaNTs could be useful in nanoelectronics, energy conversion, and separation of SWNT by chirality and size.

Acknowledgment. Financial support for this work was provided by the Robert A. Welch Foundation (C-1668), the NSF Center for Biological and Environmental Nanotechnology (EEC-0118007 and EEC-0647452), and United States Air Force Laboratory (QWD Contract No. 07-S568-0042-01-C1). We thank Laurent Cognet, Fred MacKintosh, James M. Tour, and Robert H. Hauge for helpful discussions.

References and Notes

(1) Iijima, S. *Nature* **1991**, *354*, 56.
(2) Bachtold, A.; Fuhrer, M. S.; Plyasunov, S.; Forero, M.; Anderson, E. H.; Zettl, A.; McEuen, P. L. *Phys. Rev. Lett.* **2000**, *84*, 6082.
(3) McEuen, P. L.; Fuhrer, M. S.; Park, H. K. *IEEE Trans. Nanotechnol.* **2002**, *1*, 78.
(4) Bachilo, S. M.; Strano, M. S.; Kittrell, C.; Hauge, R. H.; Smalley, R. E.; Weisman, R. B. *Science* **2002**, *298*, 2361.
(5) Baughman, R. H.; Zakhidov, A. A.; de Heer, W. A. *Science* **2002**, *297*, 787.
(6) Durkop, T.; Getty, S. A.; Cobas, E.; Fuhrer, M. S. *Nano Lett.* **2004**, *4*, 35.
(7) Carver, R. L.; Peng, H. Q.; Sadana, A. K.; Nikolaev, P.; Arepalli, S.; Scott, C. D.; Billups, W. E.; Hauge, R. H.; Smalley, R. E. *J. Nanosci. Nanotechnol.* **2005**, *5*, 1035.
(8) Parra-Vasquez, A. N. G.; Stepanek, I.; Davis, V. A.; Moore, V. C.; Haroz, E. H.; Shaver, J.; Hauge, R. H.; Smalley, R. E.; Pasquali, M. *Macromolecules* **2007**, *40*, 4043.
(9) Tans, S. J.; Devoret, M. H.; Dai, H. J.; Thess, A.; Smalley, R. E.; Geerligs, L. J.; Dekker, C. *Nature* **1997**, *386*, 474.
(10) Krupke, R.; Hennrich, F.; von Lohneysen, H.; Kappes, M. M. *Science* **2003**, *301*, 344.
(11) Barros, E. B.; Jorio, A.; Samsonidze, G. G.; Capaz, R. B.; Souza, A. G.; Mendes, J.; Dresselhaus, G.; Dresselhaus, M. S. *Phys. Rep.* **2006**, *431*, 261.
(12) Mendes, M. J.; Schmidt, H. K.; Pasquali, M. *J. Phys. Chem. B* **2008**, *112*, 7467.
(13) Duque, J. D.; Pasquali, M.; Schmidt, H. K. *J. Am. Chem. Soc.* **2008**, *130*, 15340.
(14) Buldum, A.; Lu, J. P. *Phys. Rev. Lett.* **2003**, *91*, 236801.
(15) Bonard, J. M.; Salvetat, J. P.; Stockli, T.; de Heer, W. A.; Forro, L.; Chatelain, A. *Appl. Phys. Lett.* **1998**, *73*, 918.
(16) Haga, A.; Senda, S.; Sakai, Y.; Mizuta, Y.; Kita, S.; Okuyama, F. *Appl. Phys. Lett.* **2004**, *84*, 2208.
(17) Yaish, Y.; Park, J. Y.; Rosenblatt, S.; Sazonova, V.; Brink, M.; McEuen, P. L. *Phys. Rev. Lett.* **2004**, *92*, 046401.
(18) Liu, Z.; Winters, M.; Holodniy, M.; Dai, H. J. *Angew. Chem., Int. Ed.* **2007**, *46*, 2023.
(19) Sitharaman, B.; Kissell, K. R.; Hartman, K. B.; Tran, L. A.; Baikalov, A.; Rusakova, I.; Sun, Y.; Khant, H. A.; Ludtke, S. J.; Chiu, W.; Laus, S.; Toth, E.; Helm, L.; Merbach, A. E.; Wilson, L. J. *Chem. Commun.* **2005**, 3915.
(20) Ashcroft, J. M.; Hartman, K. B.; Kissell, K. R.; Mackeyev, Y.; Pheasant, S.; Young, S.; Van der Heide, P. A. W.; Mikos, A. G.; Wilson, L. J. *J. Adv. Mater.* **2007**, *19*, 573.
(21) Cherukuri, P.; Gannon, C. J.; Leeuw, T. K.; Schmidt, H. K.; Smalley, R. E.; Curley, S. A.; Weisman, B. *Proc. Natl. Acad. Sci. U.S.A.* **2006**, *103*, 18882.
(22) Kam, N. W. S.; O'Connell, M.; Wisdom, J. A.; Dai, H. *Proc. Natl. Acad. Sci. U.S.A.* **2005**, *102*, 11600.
(23) Gannon, C. J.; Cherukuri, P.; Yakobson, B. I.; Cognet, L.; Kanzius, J. S.; Kittrell, C.; Weisman, R. B.; Pasquali, M.; Schmidt, H. K.; Smalley, R. E.; Curley, S. A. *Cancer* **2007**, *110*, 2654.
(24) Imholt, T. J.; Dyke, C. A.; Hasslacher, B.; Perez, J. M.; Price, D. W.; Roberts, J. A.; Scott, J. B.; Wadhawan, A.; Ye, Z.; Tour, J. M. *Chem. Mater.* **2003**, *15*, 3969.
(25) Ajayan, P. M.; Terrones, M.; de la Guardia, A.; Huc, V.; Grobert, N.; Wei, B. Q.; Lezec, H.; Ramanath, G.; Ebbesen, T. W. *Science* **2002**, *296*, 705.
(26) Krupke, R.; Hennrich, F.; Kappes, M. M.; v.Lohneysen, H. *Nano Lett.* **2004**, *4*, 1395.
(27) Dresselhaus, M. S.; Dresselhaus, G.; Saito, R.; Jorio, A. *Phys. Rep.* **2005**, *409*, 47.
(28) Reed, B. W.; Sarikaya, M. *Phys. Rev. B* **2001**, *64*, 195404.
(29) Reed, B. W.; Sarikaya, M.; Dalton, L. R.; Bertsch, G. F. *Appl. Phys. Lett.* **2001**, *78*, 3358.
(30) Attal, S.; Thiruvengadathan, R.; Regev, O. *Anal. Chem.* **2006**, *78*, 8098.
(31) Laverdant, J.; Buil, S.; Quelin, X. *J. Lumin.* **2007**, *127*, 176.
(32) Maier, S. A. *IEEE J. Sel. Top. Quantum Electron.* **2006**, *12*, 1214.
(33) Wang, Y.; Islam, R.; Eleftheriades, G. V. *Opt. Express* **2006**, *14*, 7279.
(34) Jiang, J.; Bosnick, K.; Maillard, M.; Brus, L. *J. Phys. Chem. B* **2003**, *107*, 9964.
(35) Redmond, P. L.; Brus, L. E. *J. Phys. Chem. C* **2007**, *111*, 14849.
(36) Kneipp, K.; Wang, Y.; Kneipp, H.; Perelman, L. T.; Itzkan, I.; Dasari, R.; Feld, M. S. *Phys. Rev. Lett.* **1997**, *78*, 1667.
(37) Maillard, M.; Huang, P. R.; Brus, L. *Nano Lett.* **2003**, *3*, 1611.
(38) Burke, P. J. *IEEE Trans. Nanotechnol.* **2003**, *2*, 55.
(39) Hao, J.; Hanson, G. W. *IEEE Trans. Nanotechnol.* **2006**, *5*, 766.
(40) Zhong, Z. H.; Gabor, N. M.; Sharping, J. E.; Gaeta, A. L.; McEuen, P. L. *Nat. Nanotechnol.* **2008**, *3*, 201.
(41) Salahuddin, S.; Lundstrom, M.; Datta, S. *IEEE Trans. Electron. Devices* **2005**, *52*, 1734.
(42) Kempa, K.; Rybczynski, J.; Huang, Z. P.; Gregorczyk, K.; Vidan, A.; Kimball, B.; Carlson, J.; Benham, G.; Wang, Y.; Herczynski, A.; Ren, Z. F. *J. Adv. Mater.* **2007**, *19*, 421.
(43) Paolucci, D.; Franco, M. M.; Iurlo, M.; Marcaccio, M.; Prato, M.; Zerbetto, F.; Penicaud, A.; Paolucci, F. *J. Am. Chem. Soc.* **2008**, *130*, 7393.
(44) Zheng, M.; Diner, B. A. *J. Am. Chem. Soc.* **2004**, *126*, 15490.
(45) O'Connell, M. J.; Eibergen, E. E.; Doorn, S. K. *Nat. Mater.* **2005**, *4*, 412.
(46) Barone, P. W.; Baik, S.; Heller, D. A.; Strano, M. S. *Nat. Mater.* **2005**, *4*, 86.
(47) Kim, S. N.; Luo, Z. T.; Papadimitrakopoulos, F. *Nano Lett.* **2005**, *5*, 2500.
(48) Zheng, M.; Rostovtsev, V. V. *J. Am. Chem. Soc.* **2006**, *128*, 7702.
(49) Alvarez, N. T.; Kittrell, C.; Schmidt, H. K.; Hauge, R. H.; Engel, P. S.; Tour, J. M. *J. Am. Chem. Soc.* **2008**, *130*, 14227.
(50) Warakulwit, C.; Nguyen, T.; Majimel, J.; Delville, M. H.; Lapeyre, V.; Garrigue, P.; Ravaine, V.; Limtrakul, J.; Kuhn, A. *Nano Lett.* **2008**, *8*, 500.
(51) Zhou, C. W.; Kong, J.; Yenilmez, E.; Dai, H. J. *Science* **2000**, *290*, 1552.
(52) Choi, H. C.; Shim, M.; Bangsaruntip, S.; Dai, H. J. *J. Am. Chem. Soc.* **2002**, *124*, 9058.
(53) Cohen, A. E.; Mahadevan, L. *Proc. Natl. Acad. Sci. U.S.A.* **2003**, *100*, 12141.
(54) Liu, J.; Dai, H. J.; Hafner, J. H.; Colbert, D. T.; Smalley, R. E.; Tans, S. J.; Dekker, C. *Nature* **1997**, *385*, 780.
(55) Martel, R.; Shea, H. R.; Avouris, P. *J. Phys. Chem. B* **1999**, *103*, 7551.
(56) Martel, R.; Shea, H. R.; Avouris, P. *Nature* **1999**, *398*, 299.
(57) Sano, M.; Kamino, A.; Okamura, J.; Shinkai, S. *Science* **2001**, *293*, 1299.

(58) Zhang, S. L.; Zhao, S. M.; Xia, M. G.; Zhang, E. H.; Xu, T. *Phys. Rev. B* **2003**, *68*, 245419.
(59) Zou, S.; Maspoch, D.; Wang; Mirkin, C. A.; Schatz, G. C. *Nano Lett.* **2007**, *7*, 276.
(60) Liu, J.; Rinzler, A. G.; Dai, H.; Hafner, J. H.; Bradley, R. K.; Boul, P. J.; Lu, A.; Iverson, T.; Shelimov, K.; Huffman, C. B.; Rodriguez-Macias, F.; Shon, Y.-S.; Lee, T. R.; Colbert, D. T.; Smalley, R. E. *Science* **1998**, *280*, 1253.
(61) Hamilton Christopher, E.; Ogrin, D.; McJilton, L.; Moore Valerie, C.; Anderson, R.; Smalley Richard, E.; Barron Andrew, R. *Dalton Trans.* **2008**, 2937.
(62) Crouse, C. A.; Maruyama, B.; Colorado Jr, R.; Back, T.; Barron, A. R. *J. Am. Chem. Soc.* **2008**, *130*, 7946.
(63) Ogrin, D.; Anderson, R. E.; Colorado, R.; Maruyama, B.; Pender, M. J.; Moore, V. C.; Pheasant, S. T.; McJilton, L.; Schmidt, H. K.; Hauge, R. H.; Billups, W. E.; Tour, J. M.; Smalley, R. E.; Barron, A. R. *J. Phys. Chem. C* **2007**, *111*, 17804.
(64) Smalley, R. E.; Li, Y.; Moore, V. C.; Price, B. K.; Colorado, R.; Schmidt, H. K.; Hauge, R. H.; Barron, A. R.; Tour, J. M. *J. Am. Chem. Soc.* **2006**, *128*, 15824.
(65) O'Connell, M. J.; Boul, P.; Ericson, L. M.; Huffman, C.; Wang, Y. H.; Haroz, E.; Kuper, C.; Tour, J.; Ausman, K. D.; Smalley, R. E. *Chem. Phys. Lett.* **2001**, *342*, 265.
(66) Sarkar, A.; Mukherjee, T.; Kapoor, S. *J. Phys. Chem. C* **2008**, *112*, 3334.
(67) Tang, X. L.; Jiang, P.; Ge, G. L.; Tsuji, M.; Xie, S. S.; Guo, Y. J. *Langmuir* **2008**, *24*, 1763.
(68) Duque, J. G.; Cognet, L.; Parra-Vasquez, A. N. G.; Nicholas, N.; Schmidt, H. K.; Pasquali, M. *J. Am. Chem. Soc.* **2008**, *130*, 2626.
(69) Pendry, J. B.; Holden, A. J.; Robbins, D. J.; Stewart, W. J. *IEEE Trans. Microwave Theory Tech.* **1999**, *47*, 2075.
(70) Bloomfield, V. A. *Biopolymers* **1991**, *31*, 1471.
(71) Vasilevskaya, V. V.; Khokhlov, A. R.; Kidoaki, S.; Yoshikawa, K. *Biopolymers* **1997**, *41*, 51.
(72) Fang, Y.; Hoh, J. H. *Nucleic Acids Res.* **1998**, *26*, 588.
(73) Schnurr, B.; MacKintosh, F. C.; Williams, D. R. M. *Europhys. Lett.* **2000**, *51*, 279.
(74) Shen, M. R.; Downing, K. H.; Balhorn, R.; Hud, N. V. *J. Am. Chem. Soc.* **2000**, *122*, 4833.
(75) Montesi, A.; Pasquali, M.; MacKintosh, F. C. *Phys. Rev. E* **2004**, *69*, 021916.
(76) Schnurr, B.; Gittes, F.; MacKintosh, F. C. *Phys. Rev. E* **2002**, *65*, 13.
(77) Thess, A.; Lee, R.; Nikolaev, P.; Dai, H. J.; Petit, P.; Robert, J.; Xu, C. H.; Lee, Y. H.; Kim, S. G.; Rinzler, A. G.; Colbert, D. T.; Scuseria, G. E.; Tomanek, D.; Fischer, J. E.; Smalley, R. E. *Science* **1996**, *273*, 483.
(78) Yakobson, B. I.; Brabec, C. J.; Bernholc, J. *Phys. Rev. Lett.* **1996**, *76*, 2511.
(79) Kudin, K. N.; Scuseria, G. E.; Yakobson, B. I. *Phys. Rev. B* **2001**, *64*, 235406.
(80) Duggal, R.; Pasquali, M. *Phys. Rev. Lett.* **2006**, *96*, 246104.
(81) Fakhri, N.; Tsyboulski, D. A.; Cognet, L.; Weisman, B.; Pasquali, M. *Proc. Natl. Acad. Sci. U.S.A.* **2009**, *106* (34), 14219−14223.
(82) Atkin, R.; Bradley, M.; Vincent, B. *Soft Matter* **2005**, *1*, 160.
(83) Brackman, J. C.; Engberts, J. *Chem. Soc. Rev.* **1993**, *22*, 85.
(84) Strano, M. S.; Huffman, C. B.; Moore, V. C.; O'Connell, M. J.; Haroz, E. H.; Hubbard, J.; Miller, M. K.; Rialon, K. L.; Kittrell, C.; Ramesh, S.; Hauge, R. H.; Smalley, R. E. *J. Phys. Chem. B* **2003**, *107*, 6979.
(85) Zanette, D.; Froehner, S. J.; Minatti, E.; Ruzza, A. A. *Langmuir* **1997**, *13*, 659.
(86) Zhai, L. M.; Lu, X. H.; Chen, W. J.; Hu, C. B.; Zheng, L. *Colloids Surf., A* **2004**, *236*, 1.

JP906038K